detritus | Multidisciplinary Journal for Circular Economy and Sustainable Management of Residues

CISA

DEVELOPMENT OF GOLD NANOSTARS DOPED FLEXIBLE SUBSTRATE FOR POLYSTYRENE MICROPLASTIC DETECTION USING SURFACE-ENHANCED RAMAN SCATTERING (SERS)

Tham Thi Hong Nguyen [1,2], Tuan Van Huynh [2], Uyen Vo Phuong Pham [1], Ngoc Bich Nguyen [1], Ly Huu Truong [1], Thang Xuan Trinh [1], Vinh Quang Lam [2,3] and Phat Trong Huynh [1,2,*]

[1] *Research Laboratories of Saigon Hi-tech Park, Ho Chi Minh city, Vietnam*
[2] *Faculty of Physics and Engineering Physics, VNUHCM, University of Science, Ho Chi Minh City, Vietnam*
[3] *Viet Nam National University HCMC, Ho Chi Minh City, Vietnam*

Article Info:
Received:
15 November 2024
Revised:
3 June 2025
Accepted:
11 June 2025
Available online:
30 June 2025

Keywords:
Microplastics
Polystyrene
Surface-enhanced Raman scattering (SERS)
Gold nanostars

ABSTRACT

Microplastics are plastic fragments smaller than 5 millimeters, originating from primary sources such as manufactured beads and fibers and secondary degradation of larger plastic materials. As a significant environmental pollutant, microplastics require sensitive and efficient detection techniques. This study presents a simple and cost-effective surface-enhanced Raman scattering method using a flexible substrate composed of gold nanostars deposited on filter paper. Polystyrene particles with an average size of approximately 0.5 µm were used as a model microplastic pollutant to evaluate the performance of the flexible substrate. The surface-enhanced Raman scattering signal enhancement was analyzed using a benchtop Raman system with a 532 nm excitation wavelength, achieving a detection limit as low as 5 µg/mL and an enhancement factor of approximately 1300. The feasibility of detecting other microplastics, including polyethylene, polypropylene and polyethylene terephthalate, was assessed. The results demonstrate that the gold nanostar-based flexible surface-enhanced Raman scattering substrate offers a highly sensitive, portable, and cost-effective alternative for real-world microplastic monitoring in aquatic environments, outperforming conventional spectroscopic techniques.

1. INTRODUCTION

Plastics have become an indispensable material in modern society due to their durability, cost-effectiveness, and versatile applications. However, their widespread use has led to the accumulation of microplastics (MPs), which are categorized into primary MPs intentionally manufactured as microbeads in cosmetics, synthetic fibers, and industrial abrasives, and secondary MPs which result from the fragmentation of larger plastic waste due to environmental factors such as UV exposure, and mechanical wear (Truong Tran Nguyen et al., 2023). MPs vary in size, shape, and chemical composition, including polystyrene (PS), polyethylene (PE), polypropylene (PP), polyethylene terephthalate (PET), and polyvinyl chloride (PVC), etc.

MPs infiltrate the environment through degradation from various sources of plastic fragmentation, such as plastic products, paint, road markings, tire dust, cosmetics, and toothpastes (Ghosh et al., 2023). Once released into the aquatic environments, MPs contaminate oceans, rivers, and even drinking water, contributing to severe pollution (Ashrafy et al., 2023). Exposure to MPs has been linked to inflammation, toxicity, and bioaccumulation, raising concerns about their long-term impacts. Studies indicate that developing countries in Southeast Asia are among the largest contributors to MPs pollution (Ng et al., 2023; Pan et al., 2024; Zhao & You, 2024).

To detect MPs in aquatic ecosystems, various analytical techniques have been developed, including optical microscopy, scanning electron microscopy (SEM), transmission electron microscopy (TEM), gas chromatography/mass spectrometry (GC-MS), and Fourier-transform infrared spectroscopy (FTIR) (Dong et al., 2023; Huang et al., 2023; Randhawa, 2023). However, these methods often suffer from limitations such as low sensitivity, high sample preparation requirements, and inability to detect small-sized MPs (Y. Zhang et al., 2023). Raman spectroscopy, particularly Surface-Enhanced Raman Scattering (SERS), has emerged as a powerful alternative due to its high sensitivity, chemical specificity, and minimal sample preparation (Chakraborty et al., 2023; Mikac et al., 2023). SERS enhances Raman signals by several orders of mag-

* Corresponding author:
Phat Trong Huynh
email: phat.huynhtrong@shtplabs.org

https://doi.org/10.31025/2611-4135/2025.19498

nitude via localized surface plasmon resonance (LSPR) in metallic nanostructures, making it suitable for detecting low concentrations of MPs (D.-Y. Lin et al., 2023; Xie et al., 2022).

Silver nanoparticles and gold nanoparticles, which have various morphologies, including nanospheres, nanorods, and nanoplates, are investigated to achieve stronger enhancement factors (EF) in SERS methods. Among these materials, gold nanostars (GNS) indicate significant improvements in Raman signal enhancement (S. Lin et al., 2019; López-Lorente, 2021). Traditionally, SERS substrates are fabricated from rigid materials such as glass and silicon; however, these substrates can be difficult to prepare due to their hydrophobic surface (Y. Zhang et al., 2023). Flexible substrates based on polydimethylsiloxane, polymethyl methacrylate, and particularly paper have received significant attention due to their low-cost, simple fabrication, ease of noble nanoparticles attachment, and compatibility with portable Raman equipment (Z. Li et al., 2020; D. Zhang et al., 2021).

In this study, we developed a flexible SERS substrate based on GNS deposited on filter paper for detecting MPs in water, focusing on polystyrene (PS) as a model MPs. Unlike conventional rigid SERS substrates (glass or silicon), our approach uses filter paper as a low-cost, flexible platform for nanoparticle deposition. By demonstrating the feasibility of GNS-based SERS detection, this study provides a method for improved real-world monitoring of MPs in environmental samples.

2. MATERIALS AND METHODS

2.1 Materials

Tetrachloroauric (III) acid ($HAuCl_4xH_2O$, ~52% Au basis), ascorbic acid ($C_6H_8O_6$, 99%), triton X-100, sodium dodecyl sulfate (SDS, 97%), trisodium citrate ($C_6H_5Na_3O_7$, 99%) and n-hexane ($CH_3(CH_2)_4CH_3$, 97%) were purchased from Sigma-Aldrich. Polystyrene powder (PS, standard sample, Mw~6.500) was from Waters. Deionized (DI) water 17.8 MΩ was used throughout the experiments. All chemical materials were GR grade.

2.2 Methods

2.2.1 Preparation of nanoparticles

Preparation of PS particles: this procedure is a modification based on a previous report (Dastbaz et al., 2021). Firstly, 0.25 g of PS powder was dissolved in 5 mL n-hexane at 50°C for 30 minutes. Subsequently, 5 mL of 0.05 M SDS was added to the mixture, which was stirred at 50°C for 60 minutes to achieve a homogeneous emulsion. Finally, the emulsion sample was placed in rotary vacuum evaporator at 50°C for 5 hours to remove n-hexane.

Preparation of gold nanostars: A mixture containing 250 µL of $HAuCl_4$ (0.01 M), 1.0 ml of aqueous 0.2 M Triton X-100 solution, 30.0 µl of $AgNO_3$ (0.01 M), and 3.75 ml DI water was stirred. Then, 250 µl of ascorbic acid (0.1 M) was added to the mixture. This mixture immediately changed from slightly yellow to colorless and cobalt, respectively, indicating formation of GNS.

2.2.2 Fabrication of flexible SERS substrates

The protocol for preparation of the flexible SERS substrate is shown in Figure 1. A 1x4 cm piece of Whatman filter paper was immersed into GNS colloidal solution in the presence of 20 mg/mL trisodium citrate (TSC) for 5 minutes. Next, the filter paper was completely dried in an oven at 37°C. The protocol has been repeated at least 10 times, resulting in the preparation of the flexible SERS substrate.

2.2.3 Characterization and SERS measurement

The spectrum of GNS was recorded using UV-Vis spectrophotometer (Jasco V-670). The micrographs of GNS and PS particles were examined by Transmission electron microscopy (Jeol-1010) and Scanning electron microscopy (Hitachi S-4800), coupled with energy-dispersive X-ray spectroscopy (EDX) for elemental analysis.

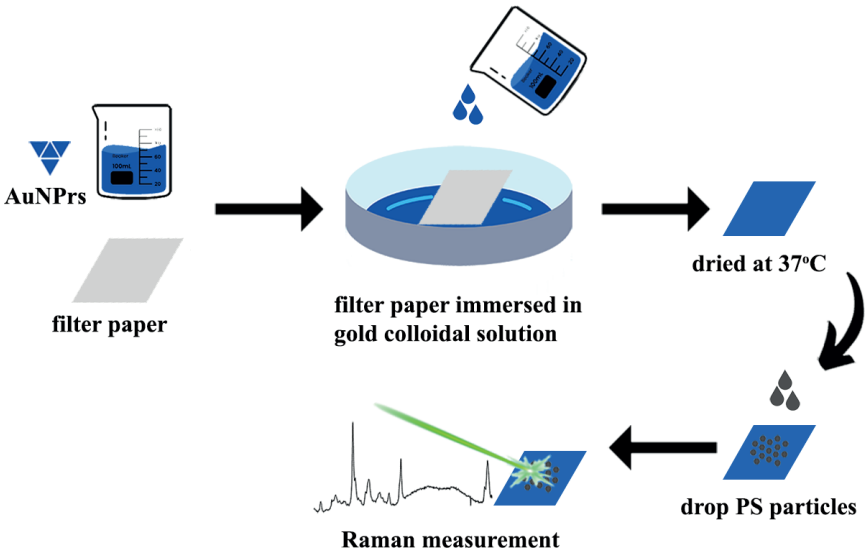

FIGURE 1: The protocol for preparation of the flexible SERS substrate.

3. RESULTS & DISCUSSION

3.1 Characterization

Figure 2 shows the characterization results of nanoparticles. Figure 2a presents the scanning electron microscopy (SEM) image of the PS particles. The image clearly shows that the PS particles are spherical in shape and have a relatively uniform size distribution, with an average particle size of approximately 0.5 µm. This is further supported by the particle size distribution histogram (Figure 2b), which indicates that most synthesized PS particles range from 350–500 nm, peaking around 400–450 nm, thus suggesting a narrow size distribution. The uniform spherical morphology of the PS particles is beneficial for several reasons. First, it ensures a consistent interaction between the PS particles and the SERS substrate, leading to more reproducible SERS measurements. Second, the size of the PS particles is environmentally relevant. Microplastics are classified into primary and secondary. Primary microplastics are those directly manufactured in that size, such as microbeads in cosmetics, while secondary microplastics result from the breakdown of larger plastic items. The 0.5 um size of the PS particles used in this study falls within the range of secondary microplastics, which are the most prevalent type found in aquatic environments, making their detection critical for assessing environmental impact (Rochman et al., 2015). Therefore, the ability of the SERS substrate to effectively detect PS particles of this size is of particular importance for environmental monitoring applications.

The optical properties of the GNS were characterized using UV-Vis spectroscopy. As shown in Figure 2c, the UV-Vis spectrum of the GNS exhibits a broad surface plasmon resonance (SPR) band centered at 635 nm, indicating that the GNS were successfully synthesized with the star-like morphology with sharp tips leading to a strong localization of the electromagnetic field at these tips, resulting in efficient SERS enhancement. The morphology of the GNS was further investigated using TEM analysis. Figure 2d shows the TEM image of the GNS, revealing that the GNS had a spherical core with a diameter of approximately 37 nm, surrounded by multiple protruding branches with an average length of 80 nm. The sharp tips of the nanostars act as "hot spots," where the electromagnetic field is greatly amplified. When the PS particles are located in close proximity to these hot spots, their Raman signals are significantly enhanced, enabling their detection at very low concentrations.

Figure 3 illustrates the analysis of the SERS substrate. The photograph of GNS (Figure 3a) attached to filter paper, where the loading of GNS is a homogeneous dark blue color, demonstrating the successful deposition of the GNS onto the substrate. The filter paper, which is a low-cost

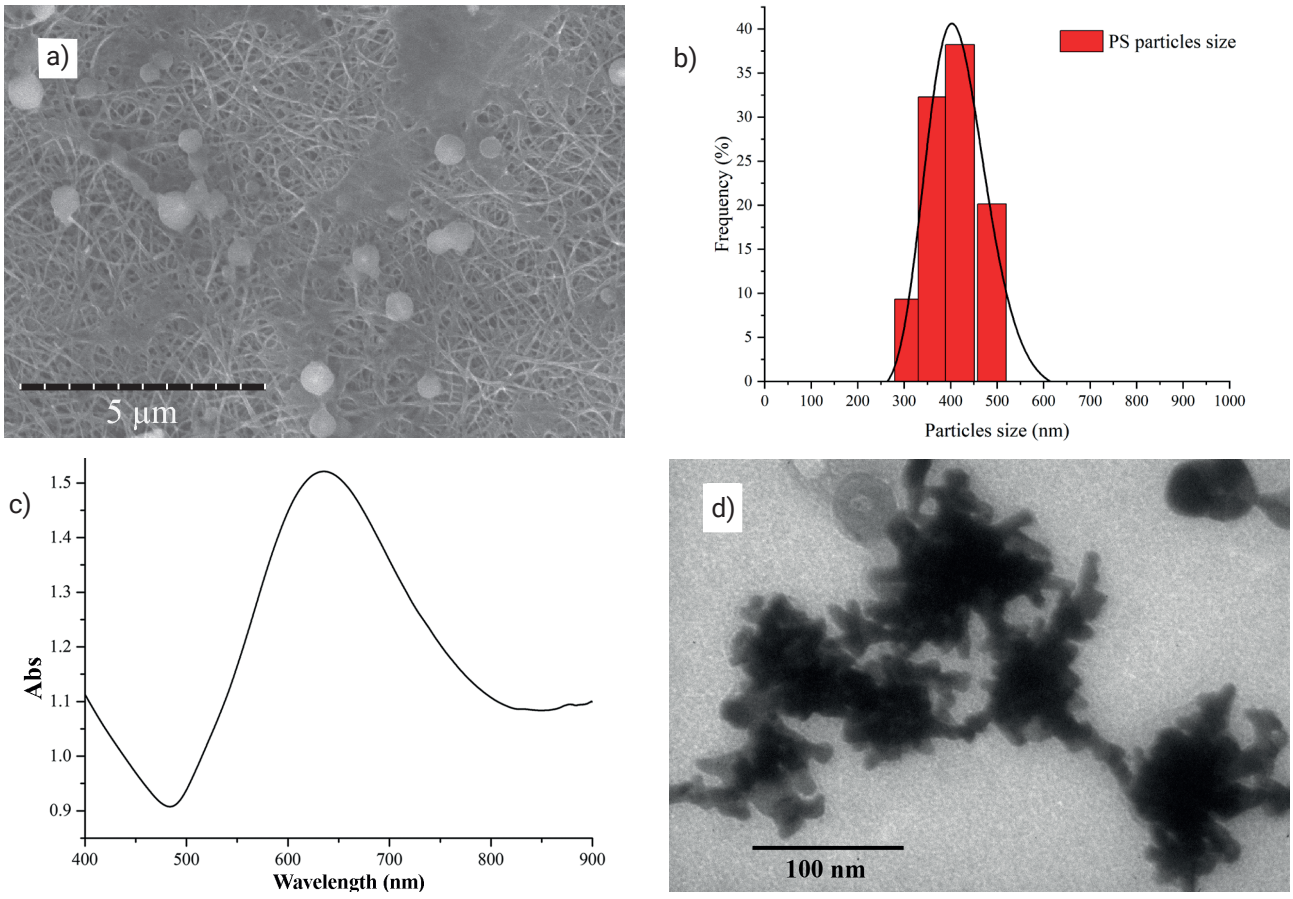

FIGURE 2: SEM image of PS particles (a); Particle size distribution of PS based on DLS (b); UV-Vis spectrum of GNS (c); TEM image of GNS (d).

and readily available material, provides a flexible and porous support for the GNS. The porosity of the filter paper allows for efficient penetration of the analyte solution, ensuring that the PS particles come into close contact with the GNS.

The distribution of the GNS on the filter paper was examined using SEM. Figures 3b and 3c show the SEM micrographs of GNS deposited on the filter paper. Figure 3b shows a low-magnification SEM image of the GNS-coated filter paper. The image reveals that the GNS are uniformly distributed on filter paper, across the entire flexible surface of the SERS substrate. This uniform distribution of the GNS is essential for achieving a consistent SERS enhancement over the entire substrate. Furthermore, the high-resolution SEM image (see Figure 3c) reveals the high density dispersion of GNS with the presence of numerous sharp tips. These sharp tips enhanced the generation of electromagnetic hot spots, leading to a significant increase in the SERS signal intensity.

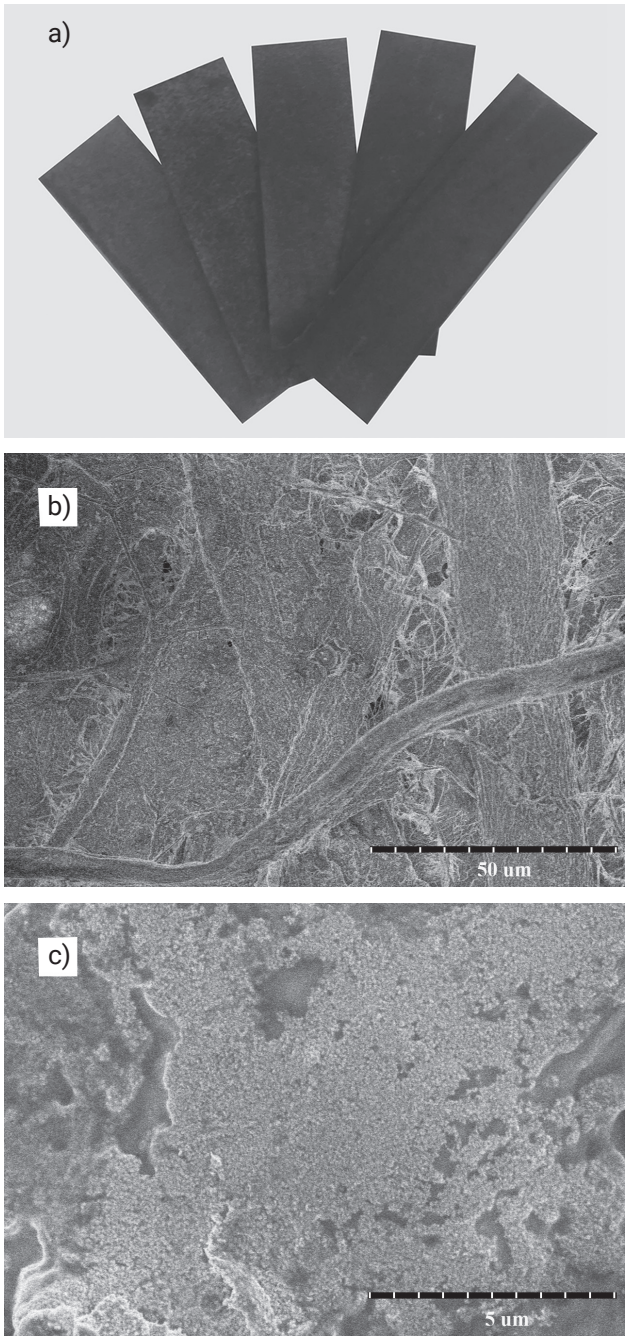

FIGURE 3: SEM image of flexible SERS substrate (a); SEM image of GNS deposited on filter paper (b); and enlarged SEM of GNS deposited on filter paper (c).

3.2 SERS performance

Figure 4 illustrates the Raman performance of polystyrene (PS) solid powder (a), normal Raman of PS particles dispersed in water at concentrations of 10 mg/mL on filter paper (b); and 200 µg/mL on a surface-enhanced Raman scattering substrate (c). In PS powder, characteristic Raman signals were identified at the following peaks: 1001 cm^{1}, corresponding to the aromatic ring C-C stretching mode; 1031 cm^{1}, attributed to C-H in-plane deformation; 1150 cm^{1}, associated with C-C stretching; 1602 cm^{1}, indicative of ring skeleton stretching; 2901 cm^{1}, related to asymmetric CH stretching; and 3051 cm^{1}, linked to aromatic CH stretching. These peaks are consistent with previously reported values for PS and serve as a spectral fingerprint for its identification (Kihara et al., 2022; Schiavi et al., 2023). The normal Raman spectra of PS particles dispersed in water at a concentration of 10 mg/mL was measured using a normal filter paper substrate. The spectrum exhibits the aromatic ring C-C stretching mode at 1001 cm^{1}, and lacked most of characteristic peaks associated with PS. In contrast, the SERS spectrum of PS particles dispersed in water at a much lower concentration of 200 µg/mL, measured using the GNS-coated flexible substrate, shows a significantly stronger signal. The peak at 1001 cm^{1} is clearly visible, and some of the other characteristic peaks of PS, such as those at 1150 cm^{1} and 1602 cm^{1}, also become apparent. This dramatic increase in signal intensity demonstrates the effectiveness of the GNS-coated flexible substrate in enhancing the Raman signal of PS particles. Consequently, the Raman peak located at 1001 cm^{-1} was selected as reference peak for the EF calculation (Xu et al., 2020).

The Raman peak at 1001 cm^{1}, corresponding to the aromatic ring C-C stretching mode, was used for the EF calculation. This peak is strong, well-defined, and consistently observed in all the spectra, making it a reliable reference for comparing the signal intensities. The EF was calculated according to the formula below, where I_{SERS} and I_{Raman} were the intensities of the normal Raman and SERS signals of the characteristic peaks as well as C_{SERS} and C_{Raman} were the concentration of PS particles dispersed in water the normal for normal Raman and SERS analytic, respectively:

$$EF = \frac{I_{SERS}}{I_{Raman}} x \frac{C_{Raman}}{C_{SERS}}$$

Figure 5 shows the “fingerprint” peaks of PS particles on SERS substrate. Various concentrations of PS particles exhibited a characteristic peak at 1001 cm^{1}, as shown in Figure 5a. The intensities corresponding to various concentrations of PS particles in water were presented in Figure 5b. The results clearly demonstrated that the intensity of the characteristic peak increased with rising concentra-

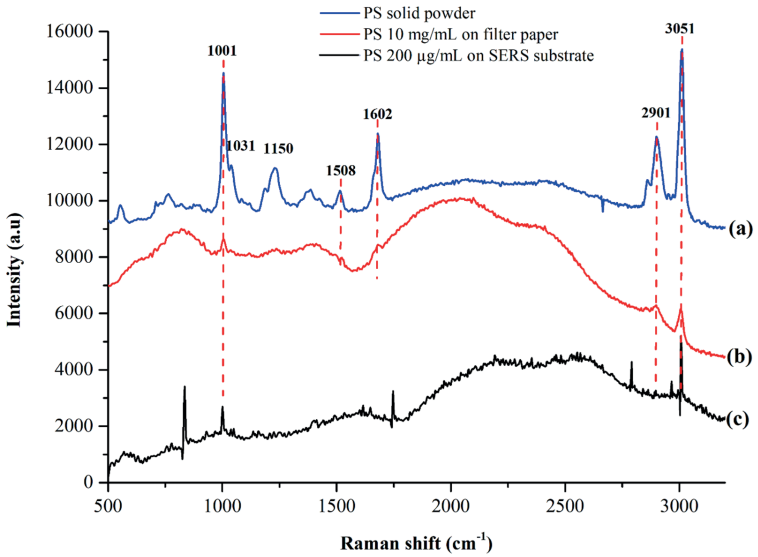

FIGURE 4: The Raman spectrum of PS solid powder (a); normal Raman of PS particles dispersed in water at concentrations of 10 mg/mL on filter paper (b); and 200 µg/mL on a surface-enhanced Raman scattering (c).

tions of PS particles. The results show that the flexible SERS substrate can detect PS particles at concentrations as low as 5 µg/mL. This detection limit is significantly lower than that of conventional Raman spectroscopy, which typically requires concentrations above 50 mg/mL for the detection of PS microplastics. The average calculated EF was approximately 1350, indicating that the SERS substrate, composed of GNS attached to filter paper, effectively enhanced the Raman signal.

The size of MPs can indeed affect their detection using GNS SERS. The SERS enhancement is most effective when the MPs are in close proximity to the GNS surface. Smaller MPs have a higher surface area-to-volume ratio, which means a larger proportion of the MP is in close contact with the GNS, leading to a stronger SERS signal. Larger MPs, on the other hand, may not interact as effectively with the GNS surface, resulting in a weaker SERS signal. However, the 0.5 um PS particles used in this study are within the optimal size range for effective SERS detection using GNS. This size is small enough to ensure close interaction with the GNS, yet large enough to provide a sufficient Raman signal. The flexible SERS substrate developed in this study has the potential to detect MPs of various sizes, but the SERS enhancement may vary depending on the size and shape of the MPs. Further research is needed to optimize the substrate for different MP sizes and shapes.

Moreover, the flexible SERS substrate developed in this study demonstrated a comparable performance to recent advancements in SERS-based microplastic detection (Liu et al., 2024; Mikac et al., 2023). These studies reported an ultrasensitive detection limit of 6.5 µg/mL for polystyrene nanoplastics using a SERS-based method, as well as a detection limit of 25 µg/mL using Ag@AuFilm SERS substrate, further confirming the effectiveness of SERS for mi-

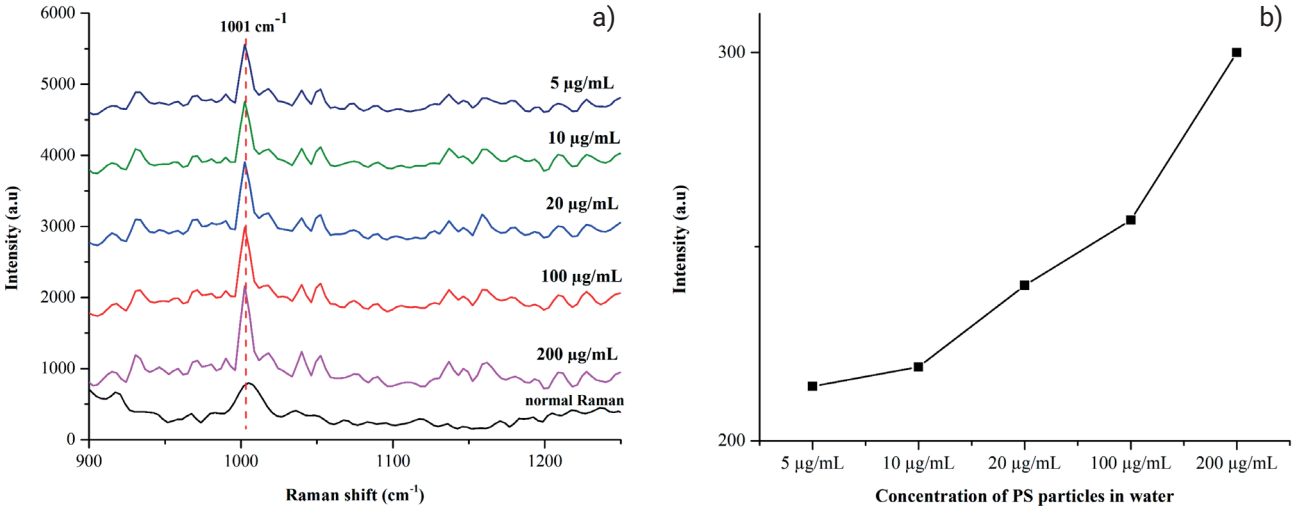

FIGURE 5: Raman spectra of various concentrations of PS particles in water on SERS substrate (a); and intensities of characteristic peak 1001 cm^{-1} (b)

croplastic analysis. These comparisons highlight the high sensitivity and practical applicability of the flexible SERS substrate developed in this work, making it a promising alternative for real-world microplastic monitoring in aquatic environments.

In addition to PS, the flexible SERS substrate was also tested for its ability to detect other common types of MPs, including PE, PP, and PET (Mallik et al., 2023; Yin et al., 2021). Preliminary results indicate that the substrate can effectively detect these microplastics as well, although the SERS enhancement efficiency may vary depending on the polymer type. The Raman spectra of PE, PP, and PET on the SERS substrate showed distinct peaks that are characteristic of each polymer, confirming their identification. However, the intensities of these peaks were generally lower than those observed for PS under the same experimental conditions. This suggests that the SERS enhancement factor may be different for different types of microplastics, possibly due to variations in their Raman scattering cross-sections, particle size, shape, and interaction with the GNS on the substrate. The stronger Raman signals observed for PS can be attributed to its aromatic rings, which resonate effectively with the excitation laser (A. Willitsford et al., 2013; A. H. Willitsford et al., 2016). Furthermore, molecules that achieve better surface adsorption through mechanisms like π-π stacking, thiol bonding, or electrostatic interaction experience greater SERS enhancement. The aromatic rings in PS facilitate a stronger interaction with noble metal surfaces via π-metal interactions (C. Li et al., 2022; Zhou et al., 2024). In contrast, PE, PP, and PET may not adsorb as as effectively. PE and PP, being made of aliphatic hydrocarbons, which have weaker Raman scattering. While PET contains aromatic components, its more complex structure may lead to less favorable orientation and interaction with the SERS substrate.

4. CONCLUSIONS

In summary, this study demonstrates the successful development of a flexible SERS substrate for the detection of PS microplastics in water. Herein, we developed a method utilizing a flexible SERS substrate in combination with a benchtop Raman spectrometer for the detection of PS particles in water, a prevalent MPs in the environment. The flexible SERS substrate, fabricated by depositing GNS onto filter paper, offers a simple, cost-effective, and sensitive method for microplastic detection. This approach enabled the detection of PS particles at a low concentrations limit of 5 µg/mL, and a high enhancement factor with an average EF over 1300 for PS particles. Thus, this method presents a cost-effective and promising procedure for the detection of MPs in aquatic environments.

ACKNOWLEDGEMENTS

This work was financially supported by Saigon Hi-tech Park under grant number: 95/2024/HĐ-QKCNC on Dec 23rd, 2024, and decision number: 11271/2023/QĐ-SKHCN on Dec 18th, 2024.

REFERENCES

Ashrafy, A. et al., (2023). Microplastics Pollution: A Brief Review of Its Source and Abundance in Different Aquatic Ecosystems. Journal of Hazardous Materials Advances, 9, 100215. https://doi.org/10.1016/j.hazadv.2022.100215

Chakraborty, I. et al., (2023). Raman spectroscopy for microplastic detection in water sources: a systematic review. International Journal of Environmental Science and Technology, 20(9), 10435-10448. 10.1007/s13762-022-04505-0

Dastbaz, Z. et al., (2021). Preparation of a stabilized aqueous polystyrene suspension via phase inversion. RSC Advances, 11(29), 17547-17557. 10.1039/D1RA02292J

Dong, H. et al., (2023). Overview of analytical methods for the determination of microplastics: Current status and trends. TrAC Trends in Analytical Chemistry, 167, 117261. https://doi.org/10.1016/j.trac.2023.117261

Ghosh, S. et al. (2023). Microplastics as an Emerging Threat to the Global Environment and Human Health. Sustainability, 15(14). doi:10.3390/su151410821

Huang, Z. et al., (2023). Analytical methods for microplastics in the environment: a review. Environmental Chemistry Letters, 21(1), 383-401. 10.1007/s10311-022-01525-7

Kihara, S. et al., (2022). Detecting polystyrene nanoplastics using filter paper-based surface-enhanced Raman spectroscopy. RSC Advances, 12(32), 20519-20522. https://doi.org/10.1039/D2RA03395J

Li, C. et al., (2022). Uncovering strong π-metal interactions on Ag and Au nanosurfaces under ambient conditions via in-situ surface-enhanced Raman spectroscopy. Chem, 8(9), 2514-2528. 10.1016/j.chempr.2022.06.008

Li, Z. et al., (2020). Recent developments of flexible and transparent SERS substrates. Journal of Materials Chemistry C, 8(12), 3956-3969. 10.1039/D0TC00002G

Lin, D.-Y. et al. (2023). Design, Fabrication, and Applications of SERS Substrates for Food Safety Detection: Review. Micromachines, 14(7). doi:10.3390/mi14071343

Lin, S. et al., (2019). Fabrication of flexible paper-based Surface-enhanced Raman scattering substrate from Au nanocubes monolayer for trace detection of crystal violet on shell. Journal of Raman Spectroscopy, 50(8), 1074-1084. https://doi.org/10.1002/jrs.5620

Liu, Y. et al., (2024). Direct detection of polystyrene microspheres by using easily fabricated Ag core embedded Au film SERS substrates with high sensitivity. Journal of Environmental Chemical Engineering, 12(5), 113311. https://doi.org/10.1016/j.jece.2024.113311

López-Lorente, Á. I., (2021). Recent developments on gold nanostructures for surface enhanced Raman spectroscopy: Particle shape, substrates and analytical applications. A review. Analytica Chimica Acta, 1168, 338474. https://doi.org/10.1016/j.aca.2021.338474

Mallik, A. et al., (2023). Study of feeding biology and diet-associated microplastic contamination in selected creek fishes of northeastern Arabian Sea: A multi-species approach. Marine Pollution Bulletin, 190, 114875. https://doi.org/10.1016/j.marpolbul.2023.114875

Mikac, L. et al., (2023). Surface-enhanced Raman spectroscopy for the detection of microplastics. Applied Surface Science, 608, 155239. https://doi.org/10.1016/j.apsusc.2022.155239

Ng, C. H. et al., (2023). Plastic waste and microplastic issues in Southeast Asia. 11. 10.3389/fenvs.2023.1142071

Pan, B. et al., (2024). Global trends and hotspots evolution in soil microplastic pollution research: A bibliometric analysis based on the Web of Science. Ecological Indicators, 161, 111974. https://doi.org/10.1016/j.ecolind.2024.111974

Randhawa, J. S., (2023). Advanced analytical techniques for microplastics in the environment: a review. Bulletin of the National Research Centre, 47(1), 174. 10.1186/s42269-023-01148-0

Rochman, C. M. et al., (2015). Anthropogenic debris in seafood: Plastic debris and fibers from textiles in fish and bivalves sold for human consumption. Scientific Reports, 5(1), 14340. 10.1038/srep14340

Schiavi, S. et al., (2023). Plasmonic Nanomaterials for Micro- and Nanoplastics Detection. Applied Sciences, 13(16). https://doi.org/10.3390/app13169291

Truong Tran Nguyen, S. et al., (2023). Riverine Microplastics Pollution in Vietnam: A Review of Current Scientific Knowledge and Legal Policies. Applied Environmental Research, 45(3). 10.35762/AER.2023014

Willitsford, A. et al., (2013). Resonance enhanced Raman scatter in liquid benzene at vapor-phase absorption peaks. Optics Express, 21(22), 26150-26161. 10.1364/OE.21.026150

Willitsford, A. H. et al., (2016). Resonance-Enhanced Raman Scattering of Ring-Involved Vibrational Modes in the 1B2u Absorption Band of Benzene, Including the Kekule Vibrational Modes v9 and v10. The Journal of Physical Chemistry A, 120(4), 503-506. 10.1021/acs.jpca.5b08159

Xie, L. et al., (2022). State of the art in flexible SERS sensors toward label-free and onsite detection: from design to applications. Nano Research, 15(5), 4374-4394. 10.1007/s12274-021-4017-4

Xu, G. et al., (2020). Surface-Enhanced Raman Spectroscopy Facilitates the Detection of Microplastics <1 μm in the Environment. Environmental Science & Technology, 54(24), 15594-15603. https://doi.org/10.1021/acs.est.0c02317

Yin, R. et al., (2021). Sensitive and rapid detection of trace microplastics concentrated through Au-nanoparticle-decorated sponge on the basis of surface-enhanced Raman spectroscopy. Environmental Advances, 5, 100096. https://doi.org/10.1016/j.envadv.2021.100096

Zhang, D. et al., (2021). Advances in flexible surface-enhanced Raman scattering (SERS) substrates for nondestructive food detection: Fundamentals and recent applications. Trends in Food Science & Technology, 109, 690-701. https://doi.org/10.1016/j.tifs.2021.01.058

Zhang, Y. et al., (2023). Fabrication of flexible SERS substrate based on Au nanostars and PDMS for sensitive detection of Thiram residue in apple juice. Spectrochimica Acta Part A: Molecular and Biomolecular Spectroscopy, 297, 122721. https://doi.org/10.1016/j.saa.2023.122721

Zhao, X., & You, F., (2024). Microplastic Human Dietary Uptake from 1990 to 2018 Grew across 109 Major Developing and Industrialized Countries but Can Be Halved by Plastic Debris Removal. Environmental Science & Technology, 58(20), 8709-8723. 10.1021/acs.est.4c00010

Zhou, G. et al., (2024). Observing π–Au Interaction between Aromatic Molecules and Single Au Nanodimers with a Subnanometer Gap by SERS. Analytical Chemistry, 96(1), 197-203. 10.1021/acs.analchem.3c03600